

# THE WILLIAMS STEP INCREASES THE STABILITY AND ACCURACY OF THE HORA TIME FILTER

AHMET GUZEL\* AND CATALIN TRENCHEA†

**Abstract.** The explicit weakly-stable second-order accurate leapfrog scheme is widely used in the numerical models of weather and climate, in conjunction with the Robert-Asselin (RA) and Robert-Asselin-Williams (RAW) time filters. The RA and RAW filters successfully suppress the spurious computational mode associated with the leapfrog method, but also weakly damp the physical mode and degrade the numerical accuracy to first-order. The recent higher-order Robert-Asselin (hoRA) time filter reduces the undesired numerical damping of the RA and RAW filters and increases the accuracy to second up-to third-order. We prove that the combination of leapfrog-hoRA and Williams' step increases the stability by 25%, improves the accuracy of the amplitude of the physical mode up-to two significant digits, effectively suppresses the computational modes, and further diminishes the numerical damping of the hoRA filter.

## 1. Introduction.

The leapfrog (LF) scheme applied to the initial value problem

$$u'(t) = f(u(t)), \quad u(0) = u_0 \tag{1.1}$$

is given by

$$u_{n+1} = u_{n-1} + 2\Delta t f(u_n), \tag{1.2}$$

where  $\Delta t$  denotes the fixed timestep, and  $u_n$  is the numerical solution approximating the exact solution  $u(t_n)$  at time  $t_n = n\Delta t$ . Also known as the midpoint rule or the explicit Nyström method, the leapfrog scheme is an explicit, three level, second-order accurate, weakly-stable, neutral time-stepping method. It is best suited for the time integration of linear oscillatory systems and is widely used in weather and climate computational models. The major weakness of the leapfrog scheme is the spurious growth of the computational mode when applied to nonlinear equations [4, 15, 17], the so-called “time splitting” instability [3, 14, 16]. There are various ways to damp

---

\*Department of Mathematics, University of Pittsburgh, Pittsburgh, PA, 15260, USA; [ahg13@pitt.edu](mailto:ahg13@pitt.edu). Partially supported by NSF Grant DMS 1522574

†Department of Mathematics, University of Pittsburgh, Pittsburgh, PA, 15260, USA; [trenchea@pitt.edu](mailto:trenchea@pitt.edu). Partially supported by NSF Grant DMS 1522574

computational mode of leapfrog scheme, see e.g. [4]. In the atmospheric sciences is common to control the computational mode by non-intrusively post-process the leapfrog scheme based legacy codes through a second-order time filter. This filter is closely related to the centered second-derivative time filter

$$\widetilde{u}_n = u_n + \gamma(u_{n+1} - 2u_n - u_{n-1}),$$

where  $u_n$  denotes the solution at time  $n\Delta t$  prior to time filtering,  $\widetilde{u}_n$  is the solution after filtering and  $\gamma$  is a positive real constant which determines the strength of the filter. The Robert-Asselin (RA) time filter, designed by Robert [12] and analyzed by Asselin [2], filters once the middle value  $u_n$  obtained by (1.2) into  $\overline{u}_n = u_n + \frac{\nu}{2}(u_{n+1} - 2u_n + \overline{u}_{n-1})$ . The combination LF-RA successfully suppresses the leapfrog scheme's computational mode, but also weakly damps the physical mode, reducing the second-order accuracy of the unfiltered leapfrog scheme to first order. It is currently used in the majority of the operational numerical weather prediction models, atmospheric general circulation models for climate simulation, ocean general circulation models, models of the fluids in rotating annulus laboratory experiments (see e.g., [16] and references therein).

Williams [1, 11, 16, 17] made a significant improvement to the RA filter, altering both values  $u_n$  and  $u_{n+1}$ , obtained by (1.2) into  $\overline{\overline{u}}_n = \overline{u}_n + \frac{\nu\alpha}{2}(u_{n+1} - 2\overline{u}_n + \overline{\overline{u}}_{n-1})$ , and  $\overline{\overline{u}}_{n+1} = u_{n+1} - \frac{\nu(1-\alpha)}{2}(u_{n+1} - 2\overline{u}_n + \overline{\overline{u}}_{n-1})$  respectively. Filtering one more time compared to RA, the RAW-filtered leapfrog scheme almost conserves the three-time-level mean of the predicted field, increases the accuracy of amplitude errors by two orders, yielding third-order accuracy, and greatly reduces the magnitude of the first-order truncation error.

Using a filter closely related to the third time-derivative, Li and Trenchea [14] introduced a higher-order Robert-Asselin (hoRA) type time filter. hoRA filters once the middle value  $u_n$  obtained by (1.2) into  $\overline{u}_n = u_n + \frac{\beta}{2}(u_{n+1} - 2u_n + \overline{u}_{n-1}) - \frac{\beta}{2}(u_n - 2\overline{u}_{n-1} + \overline{\overline{u}}_{n-2})$ . It is a linear post-process to the leapfrog scheme, which controls the undamped computational modes, and increases the numerical accuracy of the RA time filter to third-order when  $\beta = 0.4$ , yielding fourth order accuracy for the amplitude and phase speed of the physical mode [13, 14, 15].

Herein we propose an extension of the hoRA time filter, by altering both values  $u_n, u_{n+1}$  obtained by (LF) with a hoRA step and a Williams-type step. This combination further increases the stability, reduces the magnitude of the truncation error,

improves the accuracy of amplitude compared to the hoRA filtered leapfrog method, and also conserves the three-time-level mean.

The proposed hoRAW filtered leapfrog scheme applied to (1.1) is:

$$\begin{aligned} w_{n+1} &= u_{n-1} + 2\Delta t f(v_n) \\ u_n &= v_n + \frac{\alpha\beta}{2}(w_{n+1} - 2v_n + u_{n-1}) - \frac{\alpha\beta}{2}(v_n - 2u_{n-1} + u_{n-2}) \\ v_{n+1} &= w_{n+1} + \frac{\beta(\alpha-1)}{2}(w_{n+1} - 2v_n + u_{n-1}) - \frac{\beta(\alpha-1)}{2}(v_n - 2u_{n-1} + u_{n-2}) \end{aligned}$$

where the dimensionless parameters  $\beta \in [0, 1]$  and  $\alpha \in [0, 1]$ . Here  $w, v, u$  denote the unfiltered, once- and twice-filtered values respectively. The last two terms in each step can be combined as  $w_{n+1} - 3v_n + 3u_{n-1} - u_{n-2}$ , which is a finite difference approximation to the third time-derivative. The LF-hoRAW is generally second-order accurate, and third-order when  $\alpha = \frac{2+2\beta}{7\beta}$ , yielding fourth-order accuracy for the amplitude and phase speed of the physical mode (see e.g., [3]). Using a backward error analysis approach, the modified equations, we shall prove that when  $\alpha = \frac{2-\beta}{8-5\beta}$ , the LF-hoRAW method achieves sixth order accuracy in amplitude. When  $\alpha = \frac{4-12\beta+5\beta^2-2\sqrt{4+12\beta-15\beta^2+4\beta^3}}{25\beta^2-36\beta}$ , the hoRAW time filter has a 20% increase in stability compared hoRA, and the LF-hoRAW is 25% more stable than the AB3 method:  $u_{n+1} = u_n + \frac{\Delta t}{12}(23f(u_n) - 16f(u_{n-1}) + 5f(u_{n-2}))$ . The storage factor for the leapfrog scheme combined with hoRAW filter is 5. Compared with the intrusive AB3 method (three function evaluations per time iteration), the hoRAW-filtered leapfrog scheme is almost as accurate, stable and efficient, yet non-intrusive and easily implementable in existing legacy codes.

We briefly illustrate the improvement that may be achieved by the proposed hoRAW filter, when used in conjunction with the leapfrog scheme, by numerically integrating the simple harmonic motion  $\frac{d}{dt}(x(t), y(t)) = \omega(-y(t), x(t))$ , with the initial condition (1, 0) (see Figure 1.1). We compare the exact solution with the numerical solutions of LF-RA ( $\nu = 0.2$ ), LF-RAW ( $\nu = 0.2, \alpha = 0.53$ ), LF-hoRA ( $\beta = 0.1$ ) and LF-hoRAW ( $\beta = 0.1, \alpha = 0.27$ ).<sup>1</sup> The amplitude errors are significantly smaller with the hoRAW filter than with the RA, RAW and hoRA filters.<sup>2</sup> The energy of

<sup>1</sup>The chosen values yield, in the limit of good time resolution, the same damping rates of computational modes. (The damping rate of the computational mode for both LF-RA and LF-RAW is  $1 - \nu$ . The damping rates of the most unstable computational mode of LF-hoRA is  $1 - 2\beta$ . The damping rate of the most unstable computational mode of LF-hoRAW is  $\frac{2-3\beta-\alpha\beta+\sqrt{4+4\beta(\alpha-5)+(\alpha\beta+3\beta)^2}}{4}$ .)

<sup>2</sup>We note that for these parameter values, LF-RA has second-order amplitude accuracy, LF-

the oscillation  $x^2 + y^2$ , which is conserved by the continuous equations, decreases to 0 using the RA filter, decreases to 57% using the RAW filter, to 70% using hoRA, but is 99% conserved using the hoRAW filter, on the time interval  $[0, 500]$ .

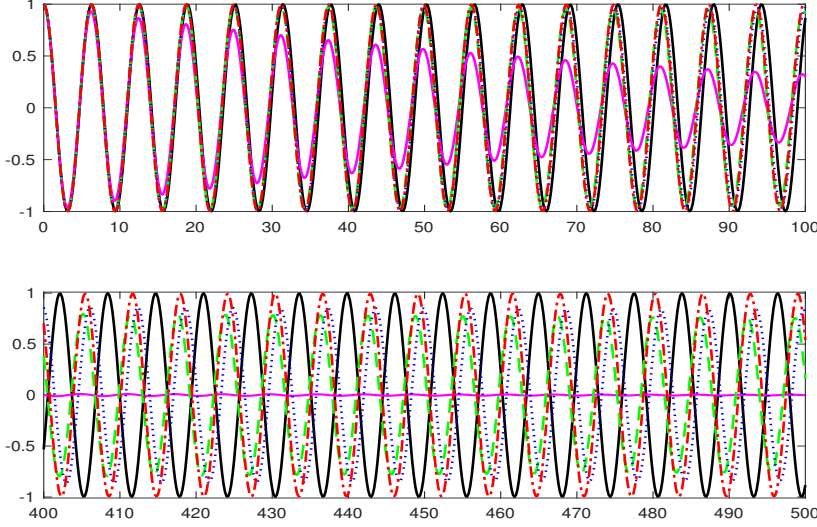


FIG. 1.1. The exact solution  $x(t)$  with  $\omega = 1 \text{ rad s}^{-1}$ , and four numerical solutions using  $\Delta t = 0.2 \text{ s}$ , on the time interval  $[0, 100]$  (top), and  $[400, 500]$  (bottom). (Exact —, LF-RA —, LF-hoRA ···, LF-RAW ---, and LF-hoRAW -.-)

The paper is organized as follows. The properties of hoRAW is characterized and analyzed in Section 2. The error analysis of phase and amplitude is given in Section 2.6 and comparison of hoRAW, hoRA and AB3 exhibited in Section 3. Some numerical tests are presented in Section 4, which support the analysis. Section 5 concludes with a summary of results.

**2. Linear Analysis.** The amplitude and phase-speed errors of time-stepping schemes for non-dissipative dynamical systems is typically evaluated by analyzing the solutions of the oscillation equation (see [4, 7]),

$$u'(t) = i\omega u(t) \quad (2.1)$$

---

RAW is almost fourth-order, LF-hoRA is fourth-order, while LF-hoRAW is sixth-order accurate in amplitude.

where  $\omega$  is real constant. In this section we derive the consistency and stability properties of the hoRAW filter. First, we briefly recall the properties of the Robert-Asselin, Robert-Asselin-Williams and hoRA time filters.

**2.1. Previous work.** The RAW-filtered leapfrog scheme applied to (2.1) writes

$$w_{n+1} = u_{n-1} + 2i\omega\Delta t v_n, \quad (\text{Leapfrog})$$

$$u_n = v_n + \frac{\alpha\nu}{2}(w_{n+1} - 2v_n + u_{n-1}). \quad (\text{Robert-Asselin})$$

$$v_{n+1} = w_{n+1} + \frac{(\alpha-1)\nu}{2}(w_{n+1} - 2v_n + u_{n-1}), \quad (\text{Williams})$$

where  $w, v, u$  are the unfiltered, once-filtered and twice-filtered values, respectively. The dimensionless parameters  $\nu \in [0, 1]$  and  $\alpha \in [0.5, 1]$ . When  $\alpha = 1$  the (Williams) step drops out and the LF-RAW becomes the LF-RA scheme, and when  $\nu = 0$  the leapfrog scheme is recovered. Both RA and RAW filters successfully dampen the computational mode, and LF-RA and LF-RAW are generally first-order accurate. However, the RAW filter provides a higher accuracy for the amplitude of the physical mode, compared to the RA filtered leapfrog (see Table 3.1). When  $\alpha = 0.5$ , the LF-RAW three-time-level mean is preserved, it is second-order accurate, yielding third-order accuracy for the amplitude of the physical mode; however LF-RAW is unconditionally unstable in this case. Nevertheless, with  $\alpha$  slightly larger than 0.5, e.g.,  $\alpha = 0.53$ , LF-RAW yields almost third-order accuracy for the amplitude of the physical mode (see [15, 16]).

The hoRA filtered leapfrog (LF-hoRA) applied to (2.1) is given by

$$v_{n+1} = u_{n-1} + 2i\omega\Delta t v_n \quad (\text{Leapfrog})$$

$$u_n = v_n + \frac{\beta}{2}(v_{n+1} - 2v_n + u_{n-1}) - \frac{\beta}{2}(v_n - 2u_{n-1} + u_{n-2}) \quad (\text{high-order RA})$$

where  $v, u$  are the unfiltered and once-filtered values, respectively, and  $\beta \in (0, 1)$ . In the limit of good time resolution, i.e.,  $\omega\Delta t \ll 1$ , the LF-hoRA scheme is generally second-order accurate, and third-order accurate when  $\beta = 0.4$  (see [14]).

**2.2. The LF-hoRAW as a linear multistep method.** The hoRAW filtered leapfrog(LF-hoRAW) scheme applied (2.1) writes as the following

$$w_{n+1} = u_{n-1} + 2i\omega\Delta t v_n \quad (\text{LF})$$

$$u_n = v_n + \frac{\alpha\beta}{2}(w_{n+1} - 2v_n + u_{n-1}) - \frac{\alpha\beta}{2}(v_n - 2u_{n-1} + u_{n-2}) \quad (\text{hoRA})$$

$$\begin{aligned} v_{n+1} = & w_{n+1} + \frac{\beta(\alpha-1)}{2}(w_{n+1} - 2v_n + u_{n-1}) \\ & - \frac{\beta(\alpha-1)}{2}(v_n - 2u_{n-1} + u_{n-2}) \end{aligned} \quad (\text{W})$$

where  $w, v, u$  are unfiltered, once filtered and twice filtered values, respectively and dimensionless parameter  $\beta \in [0, 1]$  and  $\alpha \in [0, 1]$ <sup>3</sup>. First we solve the linear system (LF)-(hoRA)-(W) for  $w_{n+1}, v_n, v_{n+1}$  in terms of  $u_n, u_{n-1}, u_{n-2}$ . Then identifying the expression for  $v_{n+1}$  with the one obtained from  $v_n$  after shifting indeces  $n \rightarrow n+1$ , we infer that the hoRAW filtered leapfrog system is equivalent to the following linear multistep method

$$\begin{aligned} u_{n+1} = & \left(\frac{\alpha\beta + 3\beta}{2}\right)u_n + (1 - 2\beta)u_{n-1} - \left(\frac{\alpha\beta - \beta}{2}\right)u_{n-2} \\ & + i\omega\Delta t((2 - \beta + \alpha\beta)u_n - 3\alpha\beta u_{n-1} + \alpha\beta u_{n-2}). \end{aligned} \quad (2.2)$$

Therefore the numerical amplification factor  $A = \frac{u_{n+1}}{u_n}$  of the LF-hoRAW method satisfies the characteristic equation

$$\begin{aligned} A^3 - & \left(\frac{\alpha\beta + 3\beta}{2} + (2 + \alpha\beta - \beta)i\omega\Delta t\right)A^2 \\ & - (1 - 2\beta - 3i\omega\Delta t\alpha\beta)A + \frac{\alpha\beta - \beta}{2} - i\omega\Delta t\alpha\beta = 0, \end{aligned} \quad (2.3)$$

with one of the three roots, the physical mode, denoted  $A_+$ , and two computational modes.<sup>4</sup> The exact solution  $u(t) = e^{i\omega t}u(0)$  of oscillation equation (2.1) has the exact amplification factor  $A_{exact} = e^{i\omega\Delta t}$ . The behaviour of the exact and numerical amplification factors of LF-hoRAW scheme in the complex plane is shown in Figure 2.1 for various  $\alpha$  and  $\beta$ . The exact amplification factor remains on the unit circle when  $\omega\Delta t$  increases from 0 to 1. One of the computational modes of LF-hoRAW is amplified when  $\omega\Delta t \geq \Sigma^{\alpha\beta}$  (see (2.5) in Section 2.4) while the physical mode  $A_+$  of LF-hoRAW stays inside the unit circle, similarly to the physical modes of AB3 [3, 4]

<sup>3</sup>The LF-hoRAW scheme reduces to LF-hoRA when  $\alpha = 1$

<sup>4</sup>The roots of (2.3) are obtained using Matlab's Symbolic Math Toolbox

and LF-hoRA [14]. The magnitudes of the physical and computational modes of LF-hoRAW are shown in Figure 2.2, for various values of  $\alpha$  and  $\beta$ . This indicates that the LF-hoRAW scheme successfully controls the growth of its computational modes, within the stability interval.

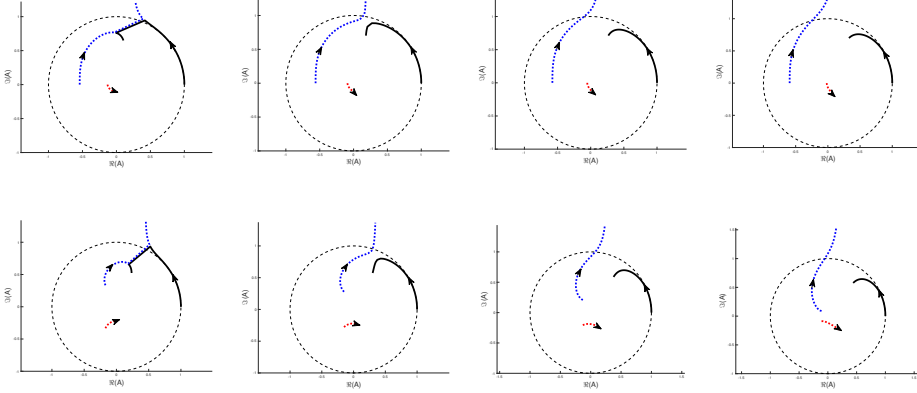


FIG. 2.1. The amplification factors of the physical mode (solid line) and two computational modes (dotted line). From left to right:  $\alpha = 0.3, 0.5, 0.7, 0.9$ , with  $\beta = 0.2$  (top) and  $\beta = 0.4$  (bottom).

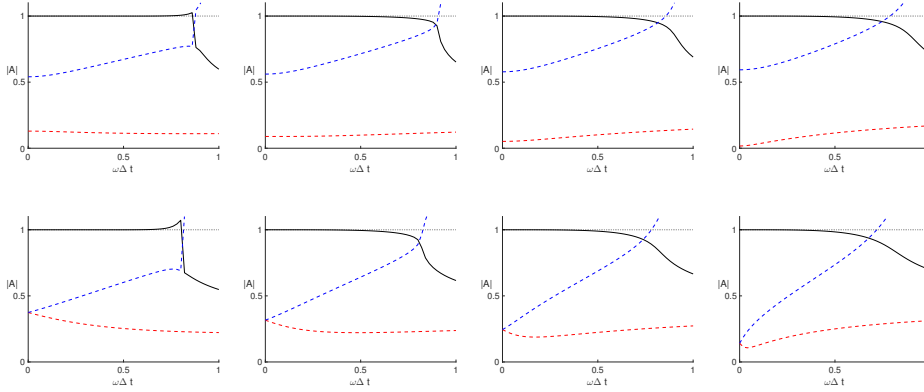


FIG. 2.2. The magnitudes of the physical mode (solid line) and computational modes (dotted line) of LF-hoRAW. From left to right:  $\alpha = 0.3, 0.5, 0.7, 0.9$ , with  $\beta = 0.2$  (top) and  $\beta = 0.4$  (bottom).

**2.3. The consistency order of LF-hoRAW.** Using the Taylor expansions of  $u(t_{n+1})$ ,  $u(t_{n-1})$  and  $u(t_{n-2})$ , the local truncation error of LF-hoRAW (2.2) writes

$$\begin{aligned}\tau_{n+1}(\Delta t) &= \frac{1}{\Delta t} \left( u(t_{n+1}) - \frac{\alpha\beta + 3\beta}{2} u(t_n) - (1 - 2\beta) u(t_{n-1}) + \frac{\alpha\beta - \beta}{2} u(t_{n-2}) \right) \\ &\quad - (2 + \alpha\beta - \beta) i\omega u(t_n) + 3\alpha\beta i\omega u(t_{n-1}) - \alpha\beta i\omega u(t_{n-2}) \\ &= \frac{2 + 2\beta - 7\alpha\beta}{6} (i\omega\Delta t)^2 u'(t_n) + \frac{28\alpha\beta - 6\beta}{24} (i\omega\Delta t)^3 u'(t_n) + \mathcal{O}((i\omega\Delta t)^4).\end{aligned}\tag{2.4}$$

Therefore the LF-hoRAW scheme is third-order accurate when  $\alpha = \frac{2+2\beta}{7\beta}$ , otherwise second-order.

**2.4. The stability domain of LF-hoRAW.** We determine the maximum interval of  $\omega\Delta t$  for which all numerical amplification factors of LF-hoRAW scheme are non-amplified using the root locus curve method [8]. The characteristic equation of LF-hoRAW (2.2) is

$$\zeta^3 - \left(\frac{\alpha\beta + 3\beta}{2}\right)\zeta^2 - (1 - 2\beta)\zeta + \left(\frac{\alpha\beta - \beta}{2}\right) - z((2 + \alpha\beta - \beta)\zeta^2 - 3\alpha\beta\zeta + \alpha\beta) = 0$$

where  $\zeta = e^{i\theta}$ ,  $\theta \in [0, 2\pi]$  represent the points on the unit circle, and  $z \in \mathbb{C}$  is the root locus curve (see Figure 2.3). The stability interval of LF-hoRAW is determined by the intersection of the imaginary axis with the root locus curve  $z$ . Setting the real of  $\zeta$  to zero gives

$$\cos(\theta) = 1 \quad \text{or} \quad \cos(\theta) = \frac{5\alpha\beta - 4\alpha - \beta + 2}{4\alpha},$$

and

$$z = 0 \quad \text{or} \quad z = \pm i \frac{(2 + \alpha\beta - \beta)\sqrt{\beta + 8\alpha - 5\alpha\beta - 2}}{2\alpha(2 - \beta)\sqrt{2 + 5\alpha\beta - \beta}},$$

which are the intersections of the root locus curve with the imaginary axis. Therefore LF-hoRAW is stable provided

$$\omega\Delta t \leq \Sigma^{\alpha\beta},$$

where

$$\Sigma^{\alpha\beta} = \frac{(2 + \alpha\beta - \beta)\sqrt{\beta + 8\alpha - 5\alpha\beta - 2}}{2\alpha(2 - \beta)\sqrt{2 + 5\alpha\beta - \beta}},\tag{2.5}$$



with  $\beta \in (0, 1)$  and  $\alpha \in (0, 1]$ . For any given  $\beta \in (0, 1)$ , the optimal value of  $\alpha$  which maximizes  $\Sigma^{\alpha\beta}$  in (2.5) is

$$\alpha^s = \frac{4 - 12\beta + 5\beta^2 - 2\sqrt{4 + 12\beta - 15\beta^2 + 4\beta^3}}{25\beta^2 - 36\beta}, \quad (2.6)$$

therefore LF-hoRAW is stable when

$$\omega\Delta t \leq \Sigma^{\alpha^s\beta} = \frac{\sqrt{2}(\sqrt{1+4\beta}+1)^{\frac{1}{2}}(17-10\beta+\sqrt{1+4\beta})^{\frac{3}{2}}}{(2-\beta)(13+5\sqrt{1+4\beta})^{\frac{3}{2}}}, \quad (2.7)$$

(see also Figure 3.3: right). From (2.5) we also note that the method becomes unstable

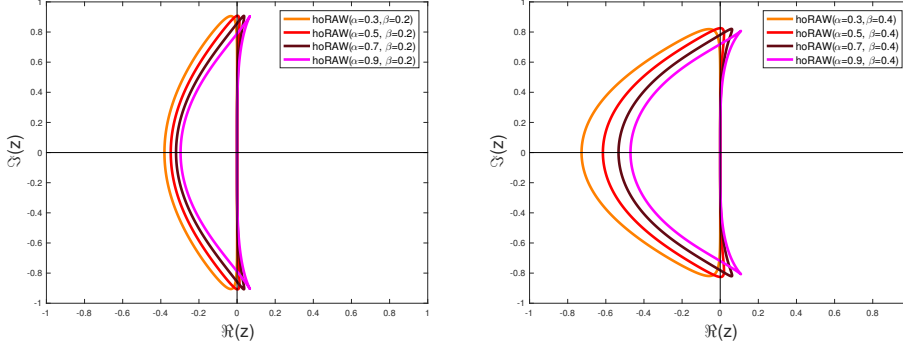


FIG. 2.3. Root locus curve of hoRAW with various  $\alpha$  and  $\beta$ .

when

$$\alpha = 1 - \frac{2}{\beta} \text{ or } \alpha = \frac{2-\beta}{8-5\beta}.$$

Since for  $\beta \in (0, 1)$  we have  $1 - \frac{2}{\beta} < 0 < \frac{2-\beta}{8-5\beta} < 1$ , henceforth we will only consider  $\alpha \in (\alpha^a, 1]$ , where

$$\alpha^a = \frac{2-\beta}{8-5\beta}. \quad (2.8)$$

We shall see in Section 2.6 that even if the scheme is unconditionally unstable when  $\alpha = \alpha^a$ , for slightly larger values  $\alpha \gtrsim \alpha^a$ , the LF-hoRAW is conditionally stable and the solution achieves sixth-order in amplitude accuracy. This phenomenon is similar to LF-RAW [16]. The amplitudes of the physical mode of LF-hoRAW are plotted in Figure 2.4 for several  $\alpha \gtrsim \alpha^a$ , and any given  $\beta$ .

**2.5. Curvature evolution.** This subsection gives a geometric interpretation of the hoRAW filter in terms of the curvature evolution [11, 13]. We define the discrete

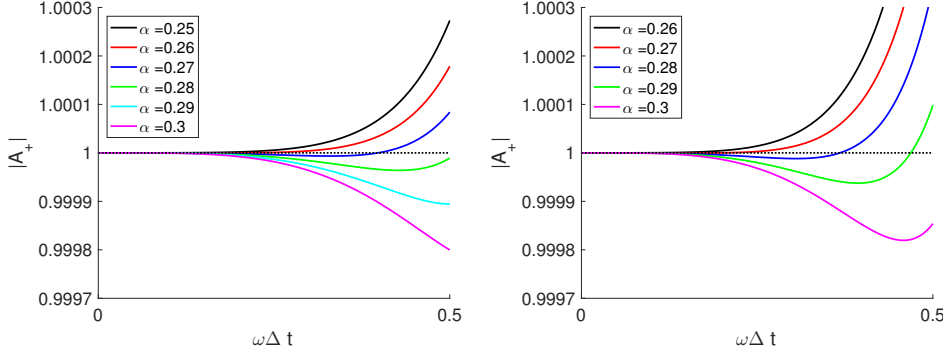


FIG. 2.4. The magnitude of physical mode amplitudes:  $\alpha \gtrsim \frac{2-\beta}{8-5\beta}$ ,  $\beta = 0.2$  (left) and  $\beta = 0.4$  (right).

curvature of  $\varphi^n$  by  $\kappa(\varphi^n) = \varphi^{n+1} - 2\varphi^n + \varphi^{n-1}$ . Two discrete curvatures are computed at every time integration of the system (1.2), one before and one after the time filter:

$$\kappa_{\text{old}}^n = w_{n+1} - 2v_n + u_{n-1}, \quad \kappa_{\text{new}}^n = v_{n+1} - 2u_n + u_{n-1}.$$

Figure 2.5 illustrates how the hoRAW time filter reduces the discrete curvature of the solution. After solving for  $w_{n+1}$  in the LF step (LF) the first solution curve is the continuous line. The curvature obtained is  $\kappa_{\text{old}}^n$ . Next, performing the (hoRA) and (W) steps leads to the new solution curve (the dashed line of Figure 2.5), with curvature  $\kappa_{\text{new}}^n$ .

The next result shows that the hoRAW filter preserves the three-level-mean of the solution curve, and decreases the discrete curvature of the solution.

PROPOSITION 2.1. *For  $n \geq 1$  we have*

$$\begin{aligned} \kappa_{\text{new}}^n &= \frac{\beta(\alpha+1)}{2} \kappa_{\text{new}}^{n-1} + \left(1 - \frac{\beta(\alpha+1)}{2}\right) \kappa_{\text{old}}^n, \\ \min\{\kappa_{\text{new}}^{n-1}, \kappa_{\text{old}}^n\} &\leq \kappa_{\text{new}}^n \leq \max\{\kappa_{\text{new}}^{n-1}, \kappa_{\text{old}}^n\} \end{aligned}$$

for all  $\alpha \in [\alpha^a, 1]$ ,  $\beta \in [0, 1]$ . When  $\alpha = \frac{1}{2}$ , the hoRAW filter preserves the three-level-mean of the solution curves

$$\frac{v_{n+1} + u_n + u_{n-1}}{3} = \frac{w_{n+1} + v_n + u_{n-1}}{3}.$$

*Proof.* The first step (hoRA) of the hoRAW filter is  $u_n = v_n + \frac{\beta\alpha}{2} \kappa_{\text{old}}^n - \frac{\beta\alpha}{2} \kappa_{\text{new}}^{n-1}$  and the second step (W) of the hoRAW filter is  $v_{n+1} = w_{n+1} + \frac{\beta(\alpha-1)}{2} \kappa_{\text{old}}^n - \frac{\beta(\alpha-1)}{2} \kappa_{\text{new}}^{n-1}$ .

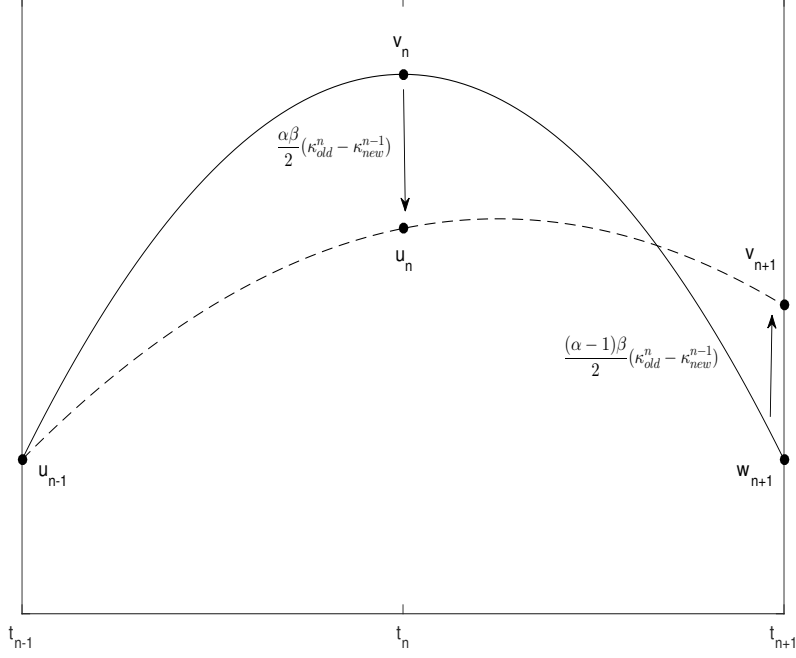


FIG. 2.5. The hoRAW filter moves the inner and right outer points through displacements  $\alpha\beta(\kappa_{old}^n - \kappa_{new}^{n-1})/2$  and  $(1-\alpha)\beta(\kappa_{old}^n - \kappa_{new}^{n-1})/2$ , respectively, where  $\alpha \in (\alpha^a, 1]$ ,  $\beta \in [0, 1]$ . The standard hoRA filter moves only the inner point through a displacement  $\beta(\kappa_{old}^n - \kappa_{new}^{n-1})/2$ .

Then

$$\begin{aligned}
 \kappa_{new}^n &= v_{n+1} - 2u_n + u_{n-1} \\
 &= (v_{n+1} - w_{n+1}) + 2(v_n - u_n) + (w_{n+1} - 2v_n + u_{n-1}) \\
 &= \frac{\beta(\alpha-1)}{2}(\kappa_{old}^n - \kappa_{new}^{n-1}) + \beta\alpha(\kappa_{new}^{n-1} - \kappa_{old}^n) + \kappa_{old}^n \\
 &= \frac{\beta(\alpha+1)}{2}\kappa_{new}^{n-1} + \left(1 - \frac{\beta(\alpha+1)}{2}\right)\kappa_{old}^n.
 \end{aligned}$$

Adding the (hoRA) and (W) steps of the hoRAW filter, for  $\alpha = \frac{1}{2}$ , yields

$$\begin{aligned}
 \frac{v_{n+1} + u_n + u_{n-1}}{3} &= \frac{w_{n+1} + v_n + \frac{\beta(2\alpha-1)}{2}\kappa_{old}^n - \frac{\beta(2\alpha-1)}{2}\kappa_{new}^{n-1} + u_{n-1}}{3} \\
 &= \frac{w_{n+1} + v_n + u_{n-1}}{3},
 \end{aligned}$$

hence the three-time-level means are preserved.  $\square$

**2.6. Error analysis.** We will derive the phase and amplitude errors of the LF-hoRAW scheme (2.2) using the notion of modified equations, an idea related to backward error analysis [6, 9, 5, 4]. The concept is to view the numerical solution of LF-hoRAW not as an approximate solution to oscillation equation (2.1), but as an exact solution to a nearby equation, called modified equation.

We define the following real constants  $C_1^{\alpha\beta}$ ,  $C_2^{\alpha\beta}$  and  $C_3^{\alpha\beta}$ , depending on  $\alpha \in [\alpha^a, 1]$ ,  $\beta \in [0, 1]$  as:

$$\begin{aligned} C_1^{\alpha\beta} &= \frac{2 + 2\beta - 7\alpha\beta}{6(2 - \beta - \alpha\beta)}, \\ C_2^{\alpha\beta} &= \frac{5\alpha\beta^2 - 8\alpha\beta + 2\beta - \beta^2}{4(2 - \beta - \alpha\beta)^2}, \\ C_3^{\alpha\beta} &= \frac{\beta^3(113\alpha^3 + 54\alpha^2 - 101\alpha + 18) - 2\beta^2(169\alpha^2 - 112\alpha + 9) + 4\beta(19\alpha - 6) - 24}{40(\alpha\beta + \beta - 2)^3}, \end{aligned} \quad (2.9)$$

and the three-term modified equation of LF-hoRAW corresponding to (2.1):

$$x'(t) = \left(1 - C_1^{\alpha\beta}(i\omega\Delta t)^2 + C_2^{\alpha\beta}(i\omega\Delta t)^3 + C_3^{\alpha\beta}(i\omega\Delta t)^4\right) i\omega x(t). \quad (2.10)$$

**PROPOSITION 2.2.** *The LF-hoRAW (2.2) is a fifth-order approximation to the modified equation (2.10)*

$$\widehat{\tau}(\Delta t) = G(x)\Delta t^5,$$

while only second-order approximation to the oscillation equation (2.1).

*Proof.* Consider a general three-term modified equation corresponding to the oscillation equation

$$y'(t) = i\omega y(t) + \Delta t^2 g_1(y(t)) + \Delta t^3 g_2(y(t)) + \Delta t^4 g_3(y(t)). \quad (2.11)$$

Then the local truncation error of LF-hoRAW (based on the modified equation, not on the oscillation equation) is

$$\begin{aligned} \widehat{\tau}_{n+1}(\Delta t) &= \frac{1}{\Delta t} \left[ y(t_{n+1}) - \left(\frac{\alpha\beta + 3\beta}{2}\right)y(t_n) - (1 - 2\beta)y(t_{n-1}) + \left(\frac{\alpha\beta - \beta}{2}\right)y(t_{n-2}) \right] \\ &\quad - (2 + \alpha\beta - \beta)i\omega y(t_n) + 3\alpha\beta i\omega y(t_{n-1}) - \alpha\beta i\omega y(t_{n-2}). \end{aligned}$$

Using the Taylor expansions of  $y(t_{n+1})$ ,  $y(t_{n-1})$ ,  $y(t_{n-2})$  at time  $t_n$ , and substitute

in  $y^{(i)}(t_n), i = 1, \dots, 5$ , the local truncation error writes

$$\begin{aligned}\widehat{\tau_{n+1}}(\Delta t) = & \left( (2 - \beta - \alpha\beta)g_1(y(t_n)) + \frac{\alpha\beta}{2}i\omega^3 y(t_n) - \frac{2 - 4\alpha\beta + 2\beta}{6}i\omega^3 y(t_n) \right) \Delta t^2 \\ & + \left( (2 - \beta - \alpha\beta)g_2(y(t_n)) + \alpha\beta i\omega g_1'(y(t_n))y(t_n) + \frac{28\alpha\beta - 6\beta}{24}\omega^4 y(t_n) \right) \Delta t^3 \\ & + \left( (2 - \beta - \alpha\beta)g_3(y(t_n)) + \alpha\beta i\omega g_2'(y(t_n))y(t_n) + \frac{\alpha\beta}{2}\omega^2 g_1(y(t_n)) \right. \\ & + \frac{\alpha\beta}{2}\omega^2 g_1'(y(t_n))y(t_n) - \frac{2 - 4\alpha\beta + 2\beta}{6}\omega^2 g_1(y(t_n)) \\ & \left. - \frac{4 - 8\alpha\beta + 4\beta}{6}\omega^2 g_1'(y(t_n))y(t_n) + \frac{2 - 81\alpha\beta + 14\beta}{120}i\omega^5 y(t_n) \right) \Delta t^4 + \mathcal{O}(\Delta t^5).\end{aligned}$$

Setting the coefficients of  $\Delta t^2$ ,  $\Delta t^3$  and  $\Delta t^4$  to zero, we obtain that  $g_1(y) = C_1^{\alpha\beta} i\omega^3 y$ ,  $g_2(y) = C_2^{\alpha\beta} \omega^4 y$  and  $g_3(y) = C_3^{\alpha\beta} i\omega^5 y$ , concluding the proof.  $\square$

Recall that the global error based on the modified equation (2.10)  $x(t_n) - u_n$  coincides with the truncation error  $\Delta t \widehat{\tau_n}(\Delta t)$ , under the localizing assumption that  $u_{n-i} = x(t_{n-i}), i = 1, 2, 3$ . Then from Proposition 2.2 we have that

$$x(t_n) - u_n = \mathcal{O}(\Delta t^6),$$

and therefore the global error of LF-hoRAW

$$u(t_n) - u_n = u(t_n) - x(t_n) + x(t_n) - u_n = u(t_n) - x(t_n) + \mathcal{O}(\Delta t^6) \quad (2.12)$$

can be characterized by the difference between the curves  $u(t)$  and  $x(t)$ .

**THEOREM 2.3.** *The phase and amplitude errors of the LF-hoRAW scheme applied to oscillation equation are*

$$\begin{aligned}R_+ - 1 &= \frac{2 + 2\beta - 7\alpha\beta}{6(2 - \beta - \alpha\beta)}(\omega\Delta t)^2 + \left[ \frac{\beta^3(113\alpha^3 + 54\alpha^2 - 101\alpha + 18)}{40(\alpha\beta + \beta - 2)^3} \right. \\ &\quad \left. - \frac{2\beta^2(169\alpha^2 - 112\alpha + 9) - 4\beta(19\alpha - 6) + 24}{40(\alpha\beta + \beta - 2)^3} \right] (\omega\Delta t)^4 + \mathcal{O}(\omega\Delta t^6), \\ |A_+| - 1 &= \frac{5\alpha\beta^2 - 8\alpha\beta + 2\beta - \beta^2}{4(2 - \beta - \alpha\beta)^2}(\omega\Delta t)^4 + \mathcal{O}(\omega\Delta t^6).\end{aligned} \quad (2.13)$$

*Proof.* With the initial conditions  $u(0) = x(0) = 1$ , the exact solution of oscillation equation (2.1) is  $u(t) = e^{i\omega t}$  and the exact solution to the modified equation (2.10)

$$\begin{aligned}x(t) &= e^{i\omega t + C_1^{\alpha\beta} i\omega^3 (\Delta t)^2 t + C_2^{\alpha\beta} \omega^4 (\Delta t)^3 t + C_3^{\alpha\beta} i\omega^5 (\Delta t)^4 t} \\ &= e^{C_2^{\alpha\beta} \omega^4 (\Delta t)^3 t} \left( \cos(\omega t + C_1^{\alpha\beta} \omega^3 (\Delta t)^2 t + C_3^{\alpha\beta} \omega^5 (\Delta t)^4 t) \right. \\ &\quad \left. + i \sin(\omega t + C_1^{\alpha\beta} \omega^3 (\Delta t)^2 t + C_3^{\alpha\beta} \omega^5 (\Delta t)^4 t) \right)\end{aligned}$$

where  $C_1^{\alpha\beta}$ ,  $C_2^{\alpha\beta}$  and  $C_3^{\alpha\beta}$  are defined in (2.10). Thus from (2.12), the phase and amplitude errors of the LF-hoRAW method in one time step are

$$R_+ - 1 = \frac{\arg(x(\Delta t))}{\arg(u(\Delta t))} - 1 = C_1^{\alpha\beta}(\omega\Delta t)^2 + C_3^{\alpha\beta}(\omega\Delta t)^4 + \mathcal{O}((\omega\Delta t)^6),$$

$$|A_+| - 1 = |x(\Delta t)| - |u(\Delta t)| = |e^{C_2^{\alpha\beta}(\omega\Delta t)^4}| - 1 = C_2^{\alpha\beta}(\omega\Delta t)^4 + \mathcal{O}((\omega\Delta t)^6),$$

in the limit of good time resolution  $\omega\Delta t \ll 1$ .  $\square$

REMARK 2.4. The phase and amplitude errors of the LF-hoRA [14] are recovered when  $\alpha = 1$ , and also the phase and amplitude errors of the Leapfrog method are recovered when  $\alpha = 1, \beta = 0$  [4].

REMARK 2.5. The LF-hoRAW method attains fourth-order accuracy in phase when  $\alpha = \frac{2+2\beta}{7\beta}$  and sixth-order accuracy in amplitude when  $\alpha = \alpha^a$ .

The amplitude and the relative phase change of the physical mode of LF-hoRAW are plotted, with various of  $\alpha$  and  $\beta$ , in Figure 2.6.

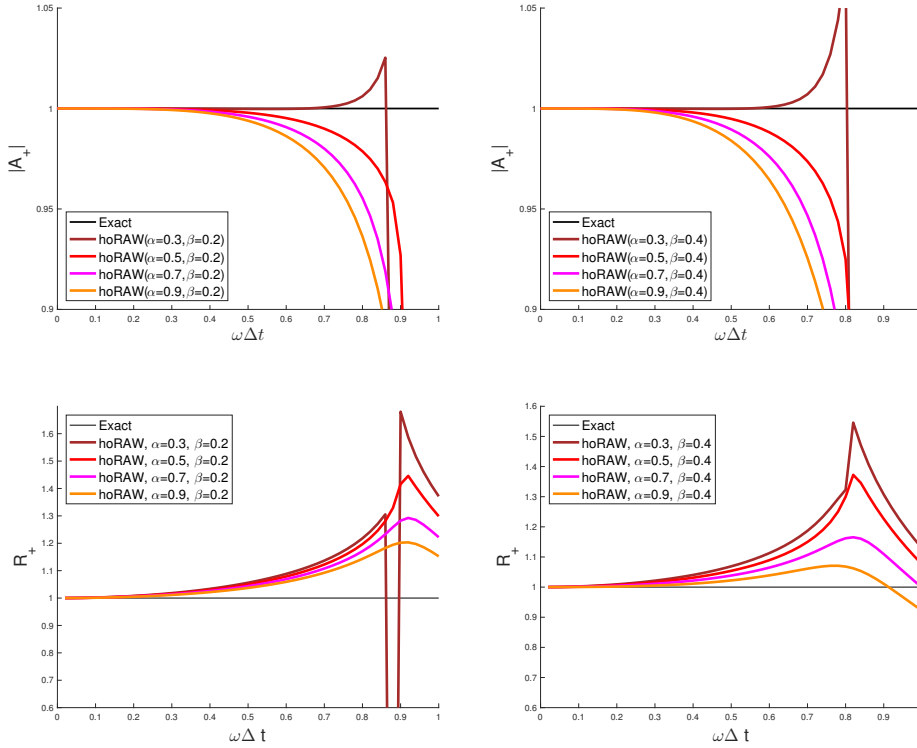


FIG. 2.6. Amplitude (top) and relative phase change (bottom) of the physical mode of hoRAW for  $\alpha = 0.3, 0.5, 0.7, 0.9$  with  $\beta = 0.2$  (left) and  $\beta = 0.4$  (right).

TABLE 2.1

Changes in amplitude, phase speed errors and stability of LF-hoRAW, for fixed, arbitrary  $\beta$ . The notation  $\nearrow, \searrow$  indicates the increase and decrease, as  $\alpha$  grows.

	$\alpha \in (\alpha^a, \alpha^s)$	$\alpha \in (\alpha^s, 1)$	Order of accuracy
Amplitude error	$\nearrow$	$\nearrow$	4
Phase-speed error	$\searrow$	$\searrow$	2, 4 if $\alpha = \frac{2+2\beta}{7\beta}$
Stability	$\nearrow$	$\searrow$	

Here is a summary of the properties of the LF-hoRAW (the case  $\alpha = 1$  corresponds to the hoRA filter) of stability, accuracy and conservation of the three-time-level mean:

$\alpha$	Conserves three time-level mean	Order of accuracy		
		Stability	Amplitude	Phase <sup>5</sup>
$= \alpha^a$ (2.8)	No	Unconditionally Unstable	6	2 (resp. 4)
$\gtrsim \alpha^a$ (2.8)	No	Conditionally Stable	4	2 (resp. 4)
1/2	Yes	Conditionally Stable	4	2 (resp. 4)
1	No	Conditionally Stable	4	2 (resp. 4)

**3. Comparison of LF-hoRA, LF-hoRAW and AB3 methods.** First we summarize the properties of the third-order methods LF-hoRA ( $\beta = 0.4$ ) [14], LF-hoRAW ( $\alpha = \frac{2+2\beta}{7\beta}, \beta \in [0, 1]$ ) and AB3 [4, 13, 14].

- The truncation errors are:

$$\tau_n(\Delta t) = \frac{11}{30}(i\omega\Delta t)^3 u'(t_n) + \mathcal{O}((i\omega\Delta t)^4) \quad (\text{hoRA}, \beta = 0.4)$$

$$\tau_n(\Delta t) = \frac{\beta+4}{12}(i\omega\Delta t)^3 u'(t_n) + \mathcal{O}((i\omega\Delta t)^4) \quad (\text{hoRAW}, \alpha = \frac{2+2\beta}{7\beta})$$

$$\tau_n(\Delta t) = \frac{3}{8}(i\omega\Delta t)^3 u'(t_n) + \mathcal{O}((i\omega\Delta t)^4) \quad (\text{AB3})$$

When  $\beta \in [0, 0.4]$ , we have that  $\frac{\beta+4}{12} \in [\frac{1}{3}, \frac{11}{30}]$ , therefore LF-hoRAW method has a smaller truncation error compared to LF-hoRA and AB3.

- The methods are stable for:

$$\omega\Delta t \leq 0.69 \quad (\text{hoRA}, \beta = 0.4)$$

$$\omega\Delta t \leq \frac{(16-5\beta)\sqrt{\beta}\sqrt{16-8\beta-3\beta^2}}{4\sqrt{3}(2-\beta)(1+\beta)\sqrt{\beta+8}} \quad (\text{hoRAW}, \alpha = \frac{2+2\beta}{7\beta})$$

$$\omega\Delta t \leq 0.72 \quad (\text{AB3})$$

<sup>5</sup>The phase is 4<sup>th</sup> order when  $\alpha = \frac{2+2\beta}{7\beta}$

The third-order methods are compared on the Lorenz system in Section 4.2.

In long-time integrations, probably the most important quantities are the stability interval and the amplitude accuracy.

We compare the accuracy of amplitude and the stability intervals of the second-order LF-hoRAW with the second and third-order LF-hoRA, and the AB3 methods in Table 3.1, with some featured values of  $\alpha$  and  $\beta$ .

The phase and amplitude of the physical mode of LF-hoRAW, LF-hoRA and AB3 are plotted in Figure 3.1. The stability regions (root locus curves) for LF-hoRAW, LF-hoRA and AB3 schemes are plotted in Figure 3.2.

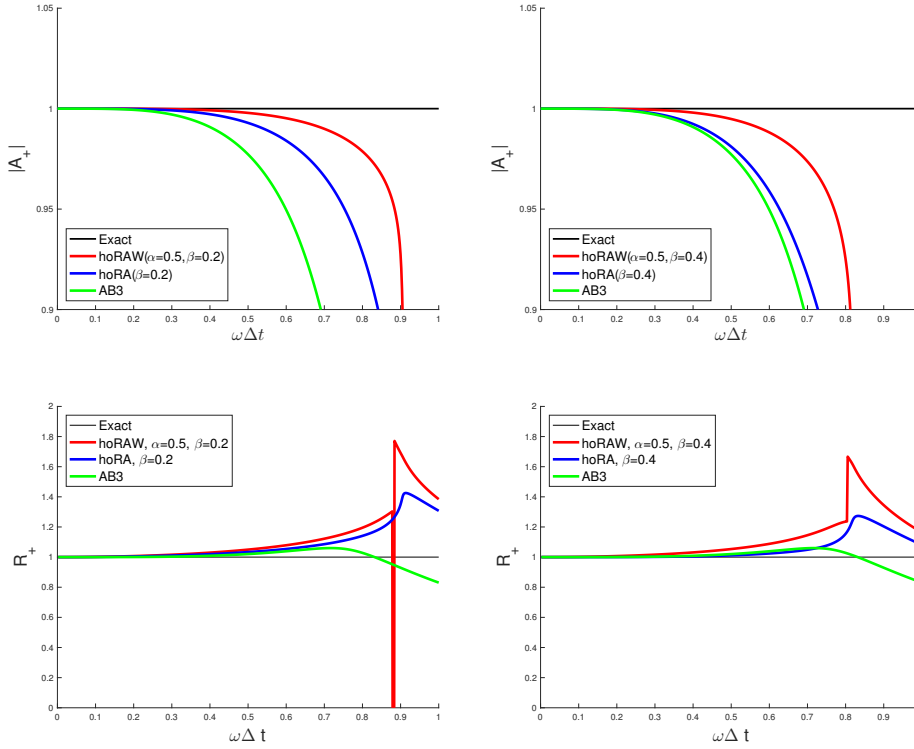


FIG. 3.1. Amplitude (top) and relative phase (bottom) of physical mode.

From the Table 3.1 and Figure 3.3 we infer that the LF-hoRAW ( $\beta = 0.2, \alpha = \alpha^s(\beta) \equiv 0.4887$ ) method exhibits about a 20% increase in stability compared to LF-hoRA method, and 25% compared to the three-level intrusive AB3 method. Moreover, the LF-hoRAW increases the amplitude accuracy by one significant digit. Also, when  $\beta = 0.2, \alpha = 0.27 \gtrsim \alpha^a(0.2) = 0.2571$  and  $\beta = 0.4, \alpha = 0.28 \gtrsim \alpha^a(0.2) = 0.2667$  the



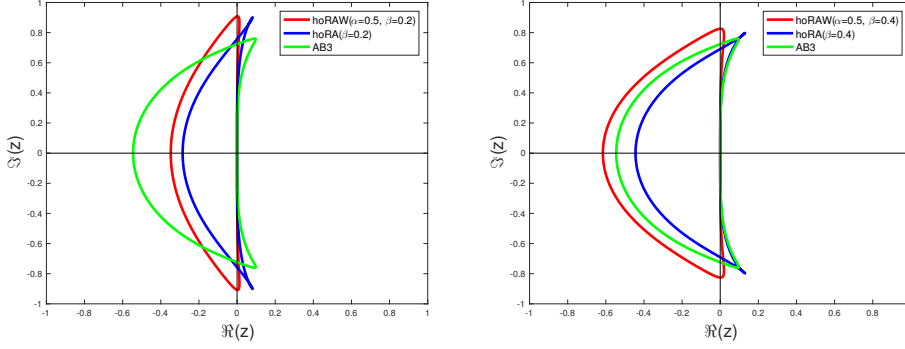


FIG. 3.2. Root locus curves of LF-hoRA, LF-hoRAW the AB3 schemes. The stability interval is given by the intersection of the root locus curve with the imaginary axis.

Method	$\beta$	$\alpha$	Order	Amplitude	Max. $\omega\Delta t$
LF	-	-	2	1	1
LF-hoRA	0.2	-	2	$1 - .1016(\omega\Delta t)^4$	0.7571
LF-hoRAW	0.2	0.27	2	$1 - .0015(\omega\Delta t)^4$	0.3977
LF-hoRAW	0.2	0.3	2	$1 - .0050(\omega\Delta t)^4$	0.6509
LF-hoRAW	0.2	0.4887	2	$1 - .0280(\omega\Delta t)^4$	0.9078
LF-hoRAW	0.2	0.5	2	$1 - .0294(\omega\Delta t)^4$	0.9075
LF-hoRA	0.4	-	3	$1 - .3056(\omega\Delta t)^4$	0.6910
LF-hoRAW	0.4	0.28	2	$1 - .0036(\omega\Delta t)^4$	0.3677
LF-hoRAW	0.4	0.3	2	$1 - .0091(\omega\Delta t)^4$	0.5402
LF-hoRAW	0.4	0.4961	2	$1 - .0701(\omega\Delta t)^4$	0.8256
LF-hoRAW	0.4	0.5	2	$1 - .0714(\omega\Delta t)^4$	0.8255
AB3	-	-	3	$1 - .3750(\omega\Delta t)^4$	0.7236

TABLE 3.1

The comparison of LF-hoRAW, LF-hoRA and AB3 methods, with some featured values of  $\beta$  and  $\alpha$  considered in Section 2.

increase in amplitude accuracy is by two significant digits.

**4. Numerical Tests.** We present three numerical tests on the LF-hoRAW, LF-hoRA and the AB3 methods. Section 4.1 shows that the hoRAW filter preserves the amplitude and phase with high accuracy.

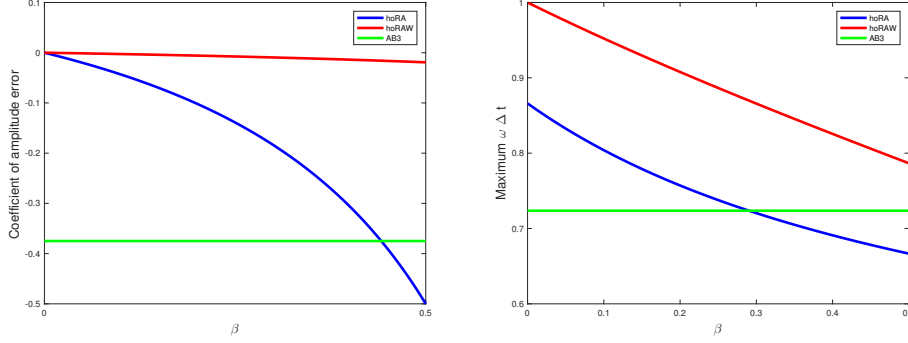


FIG. 3.3. *Left: comparison of the coefficients  $C_2^{1\beta}$ ,  $C_2^{\alpha\beta}$  (2.9) and  $C_{AB3} = \frac{3}{8}$  corresponding the LF-hoRA, LF-hoRAW and AB3 amplitude errors (2.13). Right: comparison of the maximum stability for LF-hoRA ( $\Sigma^{1\beta}$ ), LF-hoRAW (see(2.7)) and AB3 (0.7236).*

**4.1. Simple pendulum.** Consider a simple pendulum problem, given by the following two coupled nonlinear equations (see [14, 18])

$$\begin{aligned} \frac{d\theta}{dt} &= \frac{v}{L}, \\ \frac{dv}{dt} &= -g \sin \theta, \end{aligned} \tag{4.1}$$

where  $\theta, v, L$  and  $g$  denote, respectively, the angular displacement, velocity along the arc, length of the pendulum, and the acceleration due to gravity.

Set the initial condition  $(\theta(0), v(0)) = (0.9\pi, 0)$  close to the unstable equilibrium point,  $g = 9.8, L = 49$ , and numerically integrate the third-order LF-hoRA ( $\alpha = 1, \beta = 0.4$ ), the third-order AB3, and the second-order LF-hoRAW ( $\alpha = 0.3, \beta = 0.4$ ) over the time interval  $[0, 400]$ , with the time step  $\Delta t = 0.5$ . The Runge-Kutta 4 method is used to initialize the second and third steps for hoRA, hoRAW and AB3. We then compare the results with the reference solution, which computed using the adaptive RK4(5) method with the relative error tolerance  $10^{-10}$  and absolute error tolerance  $10^{-15}$ . The comparison is shown in Figure 4.1. The plots show that the LF-hoRA and AB3 damp the amplitude, and the phase errors are relatively large. The hoRAW filter preserves the amplitude and phase, with high accuracy, for a long-time period.

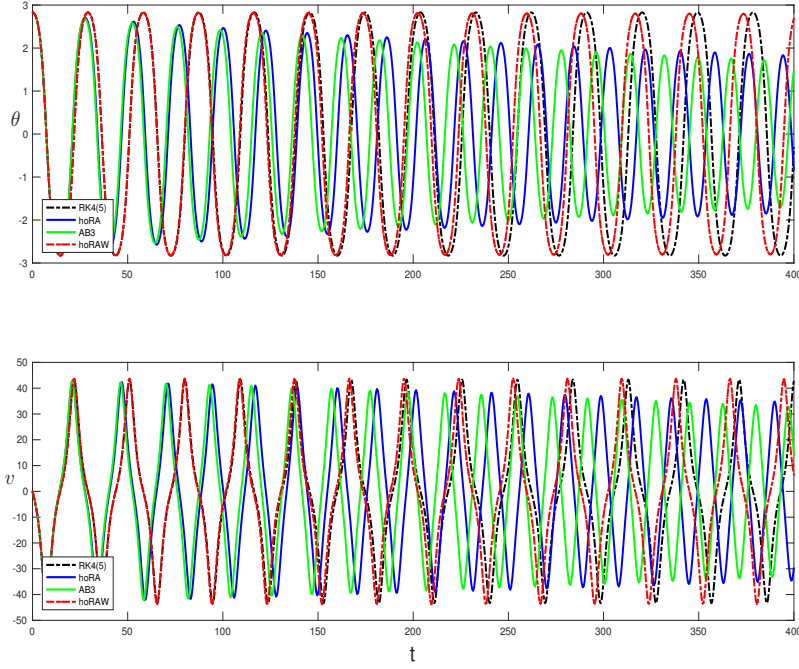


FIG. 4.1. Numerical solution to the simple pendulum problem, computed by LF-hoRA ( $\alpha = 1, \beta = 0.4$ ), AB3 and LF-hoRAW ( $\alpha = 0.3, \beta = 0.4$ ) methods, are compared with the reference solution of the adaptive RK4(5) method with relative error tolerance  $10^{-10}$  and absolute error tolerance  $10^{-15}$ . The initial condition is  $(\theta(0), v(0)) = (0.9\pi, 0)$ , and the time step is  $\Delta t = 0.5$ .

**4.2. Lorenz System.** Consider the Lorenz system:

$$\begin{aligned} \frac{dX}{dt} &= \sigma(Y - X), \\ \frac{dY}{dt} &= -XZ + rX - Y, \\ \frac{dZ}{dt} &= XY - bZ, \end{aligned} \tag{4.2}$$

with  $\sigma = 12, r = 12, b = 6$ , and the initial condition  $(X_0, Y_0, Z_0) = (-10, -10, 25)$ , as in [3, 14]. The system is numerically integrated over the time interval  $[0, 5]$  using the third-order LF-hoRAW ( $\alpha = \frac{34}{49}, \beta = 0.7$ ), the third-order LF-hoRA ( $\beta = 0.4$ ) and the third-order AB3 methods (see [3, 14]). The reference solution is computed with the adaptive RK4(5) method, using the same error tolerance as in Section 4.1. The numerical solutions of  $X$  are plotted in Figure 4.2 with various time steps  $\Delta t = 0.025, 0.029, 0.035$  and  $0.045$ .

As predicted by the linear analysis in Section 3, the third-order LF-hoRAW is as accurate the third- order LF-hoRA and AB3 methods. The augmented stability property of LF-hoRAW is exhibited as the time step is increased, pushing the LF-hoRA and AB3 to become unstable.

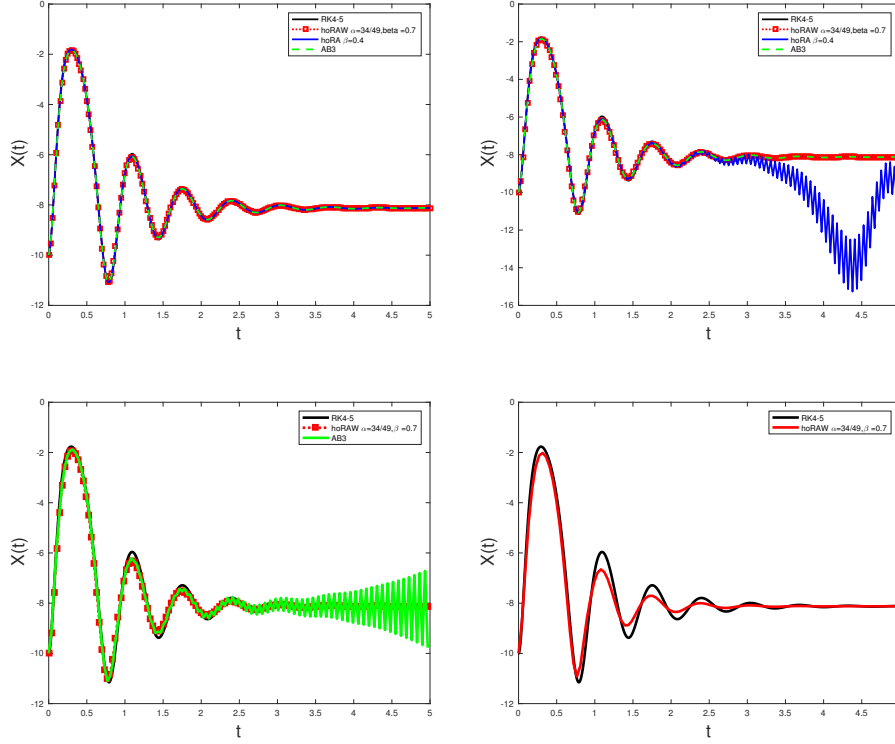
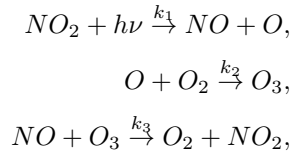


FIG. 4.2. Computed numerical solutions to the Lorenz system with LF-hoRAW( $\alpha = 37/49$ ,  $\beta = 0.7$ ), LF-hoRA( $\beta = 0.4$ ) and AB3 with constant time step  $\Delta t = 0.025$ (top left),  $\Delta t = 0.029$ (top right) and  $\Delta t = 0.035$ (bottom left),  $\Delta t = 0.045$ (bottom right).

**4.3. Ozone photochemistry.** Finally we consider a classic example from chemical reaction (see e.g., [10, 4, 14]) between atomic oxygen(O), nitrogen oxides (NO and NO<sub>2</sub>), and ozone (O<sub>3</sub>):



where  $h\nu$  denotes a photon of solar radiation. Assuming that the background concentration of  $O_2$  is constant, the concentration  $c = (c_1, c_2, c_3, c_4)$ , in molecules per cubic centimeter, of O, NO,  $NO_2$  and  $O_3$ , modeling the chemical reactions above, satisfies the system:

$$\begin{aligned}\frac{dc_1}{dt} &= k_1 c_3 - k_2 c_1, \\ \frac{dc_2}{dt} &= k_1 c_3 - k_3 c_2 c_4, \\ \frac{dc_3}{dt} &= k_3 c_2 c_4 - k_1 c_3, \\ \frac{dc_4}{dt} &= k_2 c_1 - k_3 c_2 c_4.\end{aligned}$$

We choose

$$\begin{aligned}k_1 &= 10^{-2} \max\{0, \sin(2\pi t/t_d)\} s^{-1}, \\ k_2 &= 10^{-2} s^{-1}, \quad k_3 = 10^{-16} \text{cm}^3 \text{molecule}^{-1} s^{-1},\end{aligned}$$

as in [14], where  $t_d$  is the length of 1 day in seconds, and the initial condition  $c_0 = (0, 0, 5 \times 10^{11}, 8 \times 10^{11})$  molecules  $\text{cm}^{-3}$  at  $t = 0$ . The reference solution is computed using the adaptive RK4(5) method, with the same error tolerances as before. We compare two numerical solutions, LF-hoRA( $\beta = 0.4$ ) and LF-hoRAW( $\alpha = 0.3, \beta = 0.4$ ), computed with the time step  $\Delta t = 45$  second. The chemical concentrations over the next 48 hours are shown in Figure 4.3. The LF-hoRAW method is able to capture the behaviour of concentrations with reasonable accuracy.

**5. Summary and discussion.** We have constructed and analyzed a higher-order Robert-Asselin-Williams time filter. The LF solution is once-filtered in the (hoRA) step and twice-filtered in the (W) step. The LF-hoRAW has an increased stability and accuracy of amplitude when compared to LF-RA, LF-RAW, LF-hoRA and AB3 (see Figure 1.1, and Table 3.1, Figure 3.3). The effect of the twice-filtering with the Williams' step (W) is an increase compared to the stability of LF-hoRA by almost 20%.<sup>6</sup>

The LF-hoRAW can achieve almost sixth order accuracy in amplitude ( $\alpha \gtrsim \alpha^a(\beta)$ , see (2.13) in Theorem 2.3 and (2.8)). For the specific values  $\beta = 0.2, \alpha = 0.27 \gtrsim$

---

<sup>6</sup>When  $\alpha = \alpha^s, \beta = 0$ , LF-hoRAW recovers the full-stability of LF  $\omega \Delta t \leq 1$  (unlike the hoRA filtered LF method), see e.g. Figure 3.3.

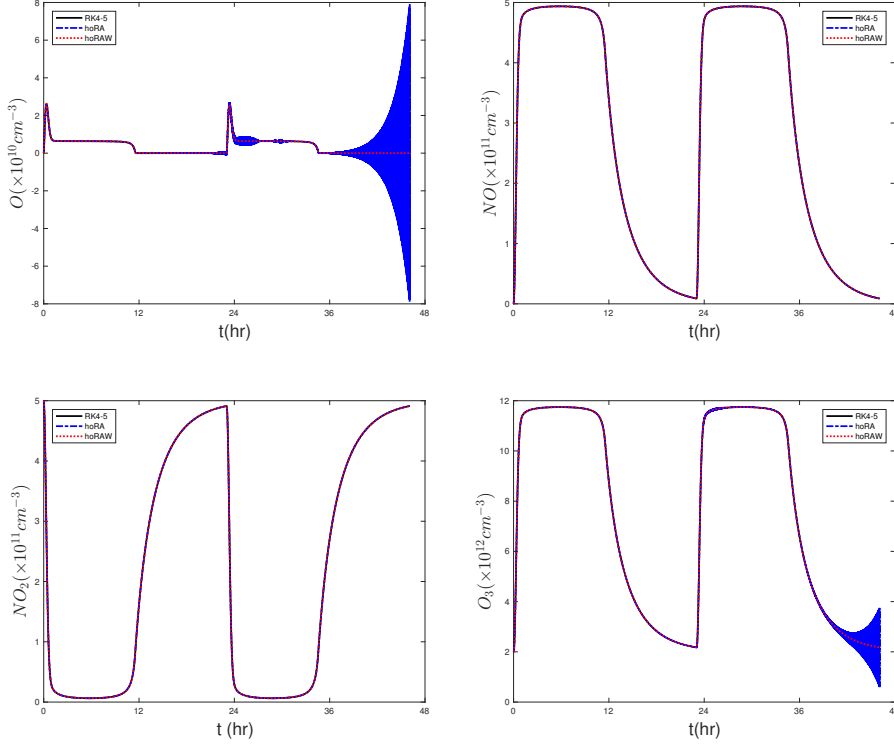


FIG. 4.3. Numerical solutions for chemical concentrations, computed using *LF-hoRAW* ( $\beta = 0.4, \alpha = 0.3$ ) and *LF-hoRA* ( $\beta = 0.4$ ), are compared with the reference solutions obtained from adaptive *RK4(5)* method with relative error tolerance  $10^{-10}$  and absolute tolerance  $10^{-15}$ . The initial condition is  $c_0 = (0, 0, 5 \times 10^{11}, 8 \times 10^{11})$  molecules  $\text{cm}^{-3}$  at  $t = 0$  with time step  $\Delta t = 45$  second.

$\alpha^a(0.2) = 0.2571$  and  $\beta = 0.4, \alpha = 0.28 \gtrsim \alpha^a(0.2) = 0.2667$ , the increase in amplitude accuracy is by two significant digits.

The hoRAW is an efficient and accurate post-process which successfully controls the growth of the computational modes and may be suitable for long-time simulations of weather and climate models.

## REFERENCES

- [1] J. AMEZCUA, E. KALNAY, AND P. D. WILLIAMS, *The effects of the RAW filter on the climatology and forecast skill of the SPEEDY model*, Mon. Wea. Rev., 139 (2011), pp. 608–619.
- [2] R. ASSELIN, *Frequency filter for time integrations*, Mon. Wea. Rev., 100 (1972), pp. 487–490.
- [3] D. R. DURRAN, *The third-order Adams-Bashforth method: An attractive alternative to leapfrog time differencing*, Mon. Wea. Rev., 119 (1991), pp. 702–720.

- [4] ———, *Numerical methods for fluid dynamics*, vol. 32 of Texts in Applied Mathematics, Springer, New York, second ed., 2010. With applications to geophysics.
- [5] D. F. GRIFFITHS AND D. J. HIGHAM, *Numerical methods for ordinary differential equations*, Springer Undergraduate Mathematics Series, Springer-Verlag London, Ltd., London, 2010. Initial value problems.
- [6] D. F. GRIFFITHS AND J. M. SANZ-SERNA, *On the scope of the method of modified equations*, SIAM J. Sci. Statist. Comput., 7 (1986), pp. 994–1008.
- [7] E. HAIRER, S. P. NØRSETT, AND G. WANNER, *Solving ordinary differential equations. I*, vol. 8 of Springer Series in Computational Mathematics, Springer-Verlag, Berlin, second ed., 1993. Nonstiff problems.
- [8] E. HAIRER AND G. WANNER, *Solving ordinary differential equations. II*, vol. 14 of Springer Series in Computational Mathematics, Springer-Verlag, Berlin, 2010. Stiff and differential-algebraic problems, Second revised edition.
- [9] N. J. HIGHAM, *Accuracy and stability of numerical algorithms*, Society for Industrial and Applied Mathematics (SIAM), Philadelphia, PA, 1996.
- [10] W. HUNSDORFER AND J. VERWER, *Numerical solution of time-dependent advection-diffusion-reaction equations*, vol. 33 of Springer Series in Computational Mathematics, Springer-Verlag, Berlin, 2003.
- [11] N. HURL, W. LAYTON, Y. LI, AND C. TRENCH, *Stability analysis of the Crank–Nicolson–Leapfrog method with the Robert–Asselin–Williams time filter*, BIT, 54 (2014), pp. 1009–1021.
- [12] M. KWIZAK AND A. J. ROBERT, *A semi-implicit scheme for grid point atmospheric models of the primitive equation*, Mon. Wea. Rev., 99 (1971), pp. 32–36.
- [13] W. LAYTON, Y. LI, AND C. TRENCH, *Recent developments in IMEX methods with time filters for systems of evolution equations*, J. Comput. Appl. Math., 299 (2016), pp. 50–67.
- [14] Y. LI AND C. TRENCH, *A higher-order Robert–Asselin type time filter*, J. Comput. Phys., 259 (2014), pp. 23–32.
- [15] ———, *Analysis of time filters used with the leapfrog scheme*, in Coupled Problems in Science and Engineering VI COUPLED PROBLEMS 2015, E. O. n. B. Schrefler and M. Papadrakakis, eds., Barcelona, Spain, april 2015, International Center for Numerical Methods in Engineering (CIMNE), pp. 1261–1272.
- [16] P. D. WILLIAMS, *A proposed modification to the Robert–Asselin time filter*, Mon. Wea. Rev., 137 (2009), pp. 2538–2546.
- [17] ———, *The RAW filter: An improvement to the Robert–Asselin filter in semi-implicit integrations*, Mon. Wea. Rev., 139 (2011), pp. 1996–2007.
- [18] ———, *Achieving seventh-order amplitude accuracy in leapfrog integrations*, Mon. Wea. Rev., 141 (2013), pp. 3037–3051.